

## Article

# Spatial–Temporal Change in Paddy Field and Dryland in Different Topographic Gradients: A Case Study of China during 1990–2020

Shuai Xie, Guanyi Yin \*, Wei Wei, Qingzhi Sun and Zhan Zhang

College of Geography and Environment, Shandong Normal University, Jinan 250358, China

\* Correspondence: 616071@sdsu.edu.cn

**Abstract:** As a country with a vast area and complex terrain, the differentiation between paddy field and dryland under different topographic gradients in China is difficult. Based on a land-use grid data set with an accuracy of 1 km, this study applied the Topographic Potential Index and used land-use transition matrices and landscape analysis to compare the change in dryland and paddy field in China from 1990 to 2020 at different elevations, slopes, and slope aspects. The results indicate that paddy field and dryland were mostly distributed in areas with better photothermal conditions. However, in recent years, the paddy field and dryland on the “sunny” slope decreased. Specifically, the area of paddy field and dryland on the southeast, south, and southwest slopes decreased, while they increased on the northwest, north, and northeast slopes. From 1990 to 2020, land conversion among paddy field, dryland, and other land use was mostly concentrated in the third ladder (<500 m elevation) of China. However, the changes in paddy field and dryland have now become active on the second ladder of China. Moreover, the change from other land to dryland on the second ladder accounted for nearly 50% of the country’s change from other land to dryland. Paddy fields and drylands in areas with low elevation and low slopes were reduced, whereas those with higher elevation and higher slopes increased, indicating that the arable land in mountainous areas increased. This indicates that the topographic conditions of arable land that become worse may aggravate soil erosion in the planting process. The landscape fragmentation of paddy field and dryland increased. Compared with paddy field, the dryland was more aggregated, the shape was more complex, and the land plots were more fragmented. As a result, paddy field and dryland show significant differences in their spatial–temporal pattern, landscape characteristics, and land-use changes, and these results can provide an important reference for the sustainable utilization of arable land resources.

**Keywords:** paddy field; dryland; topographic gradient; landscape characteristics; land-use change



**Citation:** Xie, S.; Yin, G.; Wei, W.; Sun, Q.; Zhang, Z. Spatial–Temporal Change in Paddy Field and Dryland in Different Topographic Gradients:

A Case Study of China during 1990–2020. *Land* **2022**, *11*, 1851.

<https://doi.org/10.3390/land11101851>

Academic Editors: Yongsheng Wang, Qi Wen, Dazhuan Ge and Bangbang Zhang

Received: 8 September 2022

Accepted: 14 October 2022

Published: 20 October 2022

**Publisher’s Note:** MDPI stays neutral with regard to jurisdictional claims in published maps and institutional affiliations.



**Copyright:** © 2022 by the authors. Licensee MDPI, Basel, Switzerland. This article is an open access article distributed under the terms and conditions of the Creative Commons Attribution (CC BY) license (<https://creativecommons.org/licenses/by/4.0/>).

## 1. Introduction

China is a huge nation with significant regional variations in land and water resources. Divided by the Qinling Mountains–Huaihe River line, a unique pattern of arable land use of “paddy fields in the south and drylands in the north” has formed. In the south, paddy fields account for the majority of the total area of paddy fields in China. The soil types in the south are mainly yellow–brown soil and red soil (on the Middle-Lower Yangtze Plain), lateritic red soil and latosol soil (on the Pearl River Delta Plain), purple soil and paddy soil (in the Sichuan Basin), and yellow soil (in the hilly southeastern region). The climate in the south is dominated by a tropical and subtropical monsoon climate, with an accumulated temperature of 4500–8000 °C, abundant precipitation, and sufficient heat, which forms a pattern of aquatic-based paddy farming. In the north, drylands account for the majority of the total drylands in China. The soil types are mainly Huangmian soil and Heilu soil (in the Loess Plateau), gray–brown desert soil (in Xinjiang), brown soil and cinnamon soil (in the North China Plain), and black soil and dark-brown soil (in the Northeast Plain). The warm-temperate continental monsoon climate in the north, with an

accumulated precipitation of approximately between 400 and 800 mm, forms scarce water resources, which contribute to a pattern of wheat- and maize-based dryland farming.

However, the change in paddy field and dryland is continuously dynamic and implicit, and its long-term accumulation may lead to implicit differences in arable land use. Taking the quantity and structure of paddy field and dryland in each province of China as an example, the increase in drylands and the decrease in paddy fields occurred simultaneously over the past 30 years. The province with the largest increase in paddy fields is Heilongjiang, with a cold-temperate climate in the northeast (+27,030 km<sup>2</sup>). The province with the largest increase in drylands is Xinjiang, with a dry climate in the northwest (+23,306 km<sup>2</sup>). The province with the largest decrease in both paddy fields and drylands is Guangxi Province, with fertile soil in south China (paddy fields and drylands decreased by 23,306 and 14,719 km<sup>2</sup>, respectively). In addition, relevant studies also pointed out that arable land has decreased in south China and increased in North China [1,2]. Specifically, the paddy fields increased rapidly in the northeast, whereas the drylands increased rapidly in the northwest. The spatial barycenter of paddy field and dryland in China moved northward, which indicates that the arable land moved from better agricultural areas to worse ones [3,4]. Thus, paddy fields and drylands are mostly reduced in areas with a better natural environment, while the newly added drylands and paddy fields are mostly located in areas with worse natural endowments. For example, benefited by the warm and humid climate, the Middle-Lower Yangtze Plain contributed one of highest yields of rice, wheat, and cotton in China. On the other hand, in inland Northwest China, surface water only accounts for approximately 8% of the total runoff in China because of the dry climate. The decrease in arable land in the Yangtze Plain and the increase in arable land in Northwest China shows a spatial mismatch of natural endowment and land resources. As a result, a serious spatial mismatch exists between the distribution of paddy field and dryland and the distribution of high-quality natural resources in China [5–9].

Research on the distribution patterns of paddy field and dryland has increased rapidly over the past 30 years. Previous studies mostly focused on local areas with unique geomorphological characteristics [10,11] and were devoted to analyzing the spatiotemporal change, landscape characteristics, or ecological service efficiencies of paddy field and dryland from the perspective of a single topographic element [10,12,13]. In Heilongjiang Province, Li [14] and Chen [15] found that the spatial expansion of arable land showed a strong directional trend, and the topography and geomorphology conditions were the key factors influencing the changes in paddy field and dryland. Gao [16] found that new arable and lost arable land were mainly concentrated in the plains, followed by the tablelands and hills. It was found that the drylands and paddy fields in the Loess Plateau and Chongqing city were mainly distributed at lower elevations [17,18]. By comparing land-use images from 1933, 1955, 1990, and 2005, Liu [19] found that new paddy fields in the Jinjing River of Hunan Province mainly came from woodland, which was mainly affected by topography conditions (especially elevation). By using the logit model, Zhong [20] analyzed the low mountain hilly area in southeastern China from 1999 to 2006 and found that the loss of agricultural land was the highest at low altitudes, followed by medium and high altitudes. The above studies indicate the importance of topographic factors when analyzing arable land change. Topographic differences impact the configuration of surface water, fertilizer, air, and heat, which forms the spatiotemporal differences between paddy field and dryland. Therefore, the change in paddy field and dryland on different topographic gradients should become a new tool for studying the mechanism of arable land utilization. However, in a vast area with great geographical differences, such as in China, the differentiation of long-term spatial–temporal changes in paddy field and dryland based on topographic gradients is missing.

It is crucial to study the spatial–temporal evolution and internal changes in paddy field and dryland under different topographic gradients in China. As the two major subtypes of arable land, paddy field and dryland may show different changes, further reflecting the implicit transformation of arable land use. This study refines the research perspective

of arable land use by separately observing paddy field and dryland and discusses the following questions:

I. When observing topographic conditions in terms of elevation, slope, and slope aspect, are there any differences in the spatial distribution between paddy field and dryland?

II. What is the difference in the land type changes among paddy field, dryland, and other land under different topographic conditions?

III. What do the landscape characteristics of paddy field and dryland look like from the perspective of different topographic conditions?

To address these problems, this paper took the topographic gradient as the research perspective and analyzed the spatial-temporal differentiation of two types of arable land use, paddy field and dryland, at different elevations, slopes, and slope aspects. The scientific basis for optimizing and reconstructing sustainable arable land use was provided based on the research results.

## 2. Research Methods and Data Source

### 2.1. Data Sources

This paper used land-use raster data on China with a resolution of 1 km in 1990, 1995, 2000, 2005, 2010, 2015, and 2020. These data came from the Chinese Academy of Sciences, Resource, and Environmental Science Data Center (<https://www.resdc.cn/>, accessed on 10 February 2021). The land-use raster data were established based on remote sensing satellite imagery data (Landsat 8 OLI and GF-2). Using a high-resolution remote sensing drone ground survey observation system, the spatial distribution of the land-use cover was interpreted artificially by manual visual interpretation. The testing involved a large number of samples and achieved > 94.3% accuracy [1], and such testing has played an important role in national land research. The land-use classification included six land-use types: arable land, woodland, grassland, water area, construction land, and unutilized land. These data extracted the arable land in the data set and included the two major subtypes of arable land used in the analysis: dryland and paddy field. Specifically, dryland included rain-fed land and land with irrigation facilities that grows dryland crops; paddy field contained land with irrigation facilities that grows aquatic crops.

### 2.2. The Identification of the Topographic Conditions of Paddy field and Dryland

This study used 250 m DEM raster data to calculate the elevations and slopes of paddy field and dryland using the ArcGIS Toolbox. We extracted by mask the 1 km land-use data by the reclassified DEM information to obtain the different topographic conditions of the paddy field and dryland distribution. Based on the suitability of growing staple crops, the elevations were divided into 7 gradients including 0–200, 200–500, 500–1000, 1000–1500, 1500–2500, 2500–3500, and >3500 m. Similarly, the slopes were divided into 5 grades: 0–2°, 2–6°, 6–15°, 15–25°, and >25°. The slope directions were divided into north, northeast, east, southeast, south, southwest, west, and northwest categories.

### 2.3. The Transformation between Paddy Field and Dryland

This paper calculated the land-use transformation matrix among paddy field, dryland, and other land-use types based on the toolbox in ArcGIS 10.2. The calculations were as follows:

Firstly, paddy field, dryland, and other land-use types in the  $A_{th}$  year were reclassified as 1, 2, and 3. Paddy field, dryland, and other land-use types in the  $B_{th}$  year were reclassified as 10, 20, and 30.

Secondly, the land-use layers of the  $A_{th}$  year and the  $B_{th}$  year were summed in the raster calculator, and the attribute data of the newly exported layer indicated the number of rasters that changed from one land-use type in the  $A_{th}$  year to another one in the  $B_{th}$  year. For instance, 12 indicates the land-use change from a paddy field in the  $A_{th}$  year to dryland in the  $B_{th}$  year. Detailed attributed data and the implication of the land-use change are listed in Table 1.

Thirdly, the total area of land changed from one land-use type to another was calculated by multiplying the number of the changed rasters by the area of the rasters (i.e., 1 km<sup>2</sup> in this study).

**Table 1.** The attribute data and the implication of the land-use change.

Grid Value	Implication	Grid Value	Implication
11	Unchanged paddy field	22	Unchanged dryland
12	Paddy field→Dryland	21	Dryland→Paddy field
13	Paddy field→Other land	23	Dryland→Other land
31	Other land→Paddy field	32	Other land→Dryland

#### 2.4. The Landscape Characteristics of Paddy Field and Dryland

In land use, different land units combine into different spatial patterns such as land patch densities, shape characteristics, and aggregation degrees. These features constitute the landscape differences between paddy field and dryland. This paper evaluated the landscape characteristic of paddy field and dryland in terms of three aspects: intensity, shape, and vergence. Eight indexes were further analyzed: patch number, landscape aggregation degree, etc. (Table 2). By importing the raster data of paddy field and dryland into Fragstats software, this study calculated the values of the landscape indexes of paddy field and dryland from 1990 to 2020 [21,22].

**Table 2.** Introduction of the landscape indexes.

Categories	Indexes	Title	Introduction
Intensity	NP	Number of patches	NP is the total number of all patches in the landscape, which can reflect the landscape spatial pattern.
	PD	Patch density	PD is the number of patches per unit area.
	LPI	Largest patch index (%)	LPI is the proportion of the largest patch of a land-use type in the whole landscape, which is used to measure the characteristics of the dominant landscape patches.
Shape	LSI	Landscape shape index	LSI is the shape complexity of arable land patches, which was measured by the deviation of the shape of the land patch from a circle or a square of the same area.
	AWMSI	Area-weighted mean shape index	AWMSI is the sum of the average shape factor of each land patch multiplied by the weight (the land patch area in the total landscape area). Bigger landscape patches have a higher weight than smaller patches.
Vergence	AI	Aggregation index (%)	AI refers to the aggregation degree of the landscape based on the common boundary length of patches of the same type of landscape.
	DIVISION	Landscape isolation	DIVISION refers to the individual isolated distribution of different patches in the landscape types.
	SPLIT	Splitting Index	SPLIT refers to the ratio of landscape fragmentation to the total landscape area index, which is used to describe the dispersion of the landscape pattern.

#### 2.5. Topographic Potential Index

Because the distribution of land-use types is highly related to elevation and slope, this paper adopts the Topographic Position Index composed of slope and elevation to reflect the comprehensive topographic features of the paddy field and dryland.

$$TPI = \lg \left[ \left( \frac{E}{E_0} + 1 \right) * \left( \frac{S}{S_0} + 1 \right) \right] \quad (1)$$

where *TPI* refers to the Topographic Potential Index; *E* and *E*<sub>0</sub> are the elevation and the average elevation of an area, respectively; *S* and *S*<sub>0</sub> are the slope and the average slope of an area, respectively. The *T* value increases along with the increase in slope and elevation.

When the slope increases while the elevation decreases, or when the elevation increases while the slope decreases, the value of *TPI* is in the middle of the two. Referring to the relevant literature [23], this paper classified the topographic position index (abbreviated as *TPI*) into three levels: high ( $>0.8$ ), medium ( $0.4\text{--}0.8$ ), and low ( $<0.4$ ).

### 3. Result Analysis

#### 3.1. Changes in the Topographic Characteristics of Paddy Field and Dryland

The results showed some similarities in the distribution of the *TPI* of paddy field and dryland (Figure 1). Firstly, paddy fields and drylands with a low *TPI* were mainly distributed in the low-elevation areas of eastern China. Specifically, the paddy fields with a low *TPI* were mainly distributed in the Yangtze Plain areas (including Jiangsu, Shanghai, Anhui, Zhejiang, Hunan, Hubei, and Sichuan), the southern areas of China (Guangdong and Taiwan), the northeastern area (Liaoning and Heilongjiang), and the northeast area (Ningxia Province), while the drylands with a low *TPI* were mainly distributed in the northern area (Shandong, Henan, Hebei, and Shaanxi provinces), the northeastern area (Liaoning, Jilin, Heilongjiang, and Inner Mongolia provinces), the northwestern area (Xinjiang), and the southern area (Guangdong Province). Secondly, the paddy fields and drylands with a medium *TPI* were mainly scattered in the second ladder (1000–2000 m elevation) area and small parts of the first ladder ( $>4000$  m elevation) and third ladder ( $<500$  m elevation) in China. Specifically, the paddy fields with a medium *TPI* were distributed in the south of Shaanxi Province, and the drylands were distributed in Shaanxi, Shanxi, Gansu, Ningxia, Chongqing, Sichuan, Guizhou, Guangxi, Yunnan, and other provinces. Thirdly, the paddy fields and drylands with a high *TPI* were scattered in the southwest of China, and the drylands area far surpassed that of paddy fields.

An obvious change occurred in the topographic condition of arable land. The paddy fields with a low *TPI* decreased (Table S1 in the Supplementary Materials), while the paddy fields and drylands with a medium and high *TPI* increased. Specifically, the proportion of paddy fields with a low *TPI* decreased from 86.9% to 84.9%, and the proportion of drylands with a low *TPI* decreased from 76.5% to 75.4%. Because the low *TPI* areas are mainly distributed in the third ladder of China, which is flat and low in elevation, the hydrothermal conditions and the development degree of its paddy fields and drylands are better, the loss of paddy fields and drylands with a low *TPI* due to the fact of urban expansion is regrettable, which may lead to a further decline in the suitability of agricultural production [24].

From the perspective of elevation (Figure 2), 40% of the drylands and 64% of paddy fields were distributed at 0–200 m elevation, which decreased over time. The dryland area was greater than that of paddy field at the same elevation. From 1990 to 2020, the most obvious change in dryland and paddy field was concentrated at an elevation of 0–200 m. When looking at the change in dryland, this study found that the dryland increased in all elevations except for 0–200 m, with the highest annual growth rate (1.01%) in the  $>3500$  m elevation area and the lowest annual growth rate (0.03%) in the 1500–2500 m elevation area. When looking at the change in paddy field, the results showed that the paddy field area increased at 200–500 m, 2500–3500 m, and  $>3500$  m elevations but decreased at the other elevations, with the highest average annual growth rate (2.25%) at  $>3500$  m elevations and the lowest average annual growth rate (0.01%) at 200–500 m elevations.

In terms of the slope condition (Figure 3), most of the paddy fields and drylands were concentrated at the  $0\text{--}2^\circ$  slope and decreased along with the increase in the slopes. From 1990 to 2020, paddy fields and drylands gradually moved from lower to higher slopes; the area of paddy fields and drylands in flatter areas ( $0\text{--}6^\circ$  slope) decreased, whereas the area of paddy fields and drylands in areas with a slope  $> 6^\circ$  increased. When looking at the change trends, dryland showed a fluctuating change (first increased and then decreased at  $0\text{--}2^\circ$  and  $2\text{--}6^\circ$  slopes), while paddy field showed a steadily decreasing trend at  $0\text{--}2^\circ$  and  $2\text{--}6^\circ$  slopes. When looking at the obvious change, dryland changed the most at a  $6\text{--}15^\circ$  slope (increased by 15,026 km<sup>2</sup>), whereas the paddy field area changed the most at a  $0\text{--}2^\circ$

slope (decreased by 18,846 km<sup>2</sup>). When looking at the fastest change, the dryland area and paddy field area increased the fastest (0.6% and 1.09% a year) at a slope of >25°. In summary, the increase in sloping arable land changed significantly, and the emergence of steeply sloping paddy fields and dryland is especially alarming. Because sloping paddy field and dryland have limits regarding soil and water conservation [17], to guarantee the crop yield sustainably, more slope treatment practices, such as drainage ditches, protection forest, silt arresters, and contour ploughing (terrace field), are needed in this area.

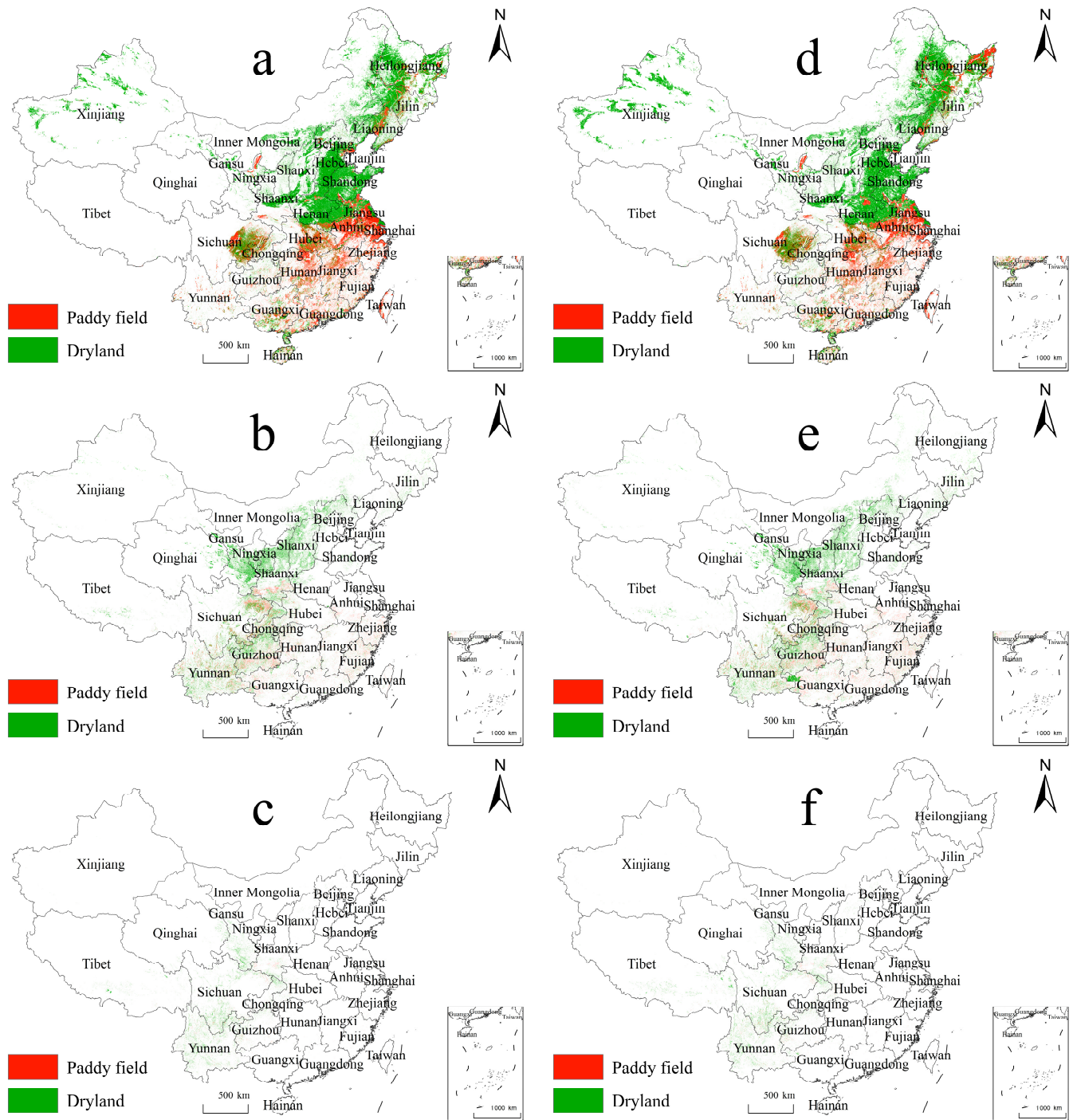


**Figure 1.** Distribution of paddy field and dryland under different TPIs in China in 1990 and 2020. ((a), low (<0.4) TPI in 1990; (b), medium (0.4–0.8) TPI in 1990; (c), high (>0.8) TPI in 1990; (d), low (<0.4) TPI in 2020; (e), medium (0.4–0.8) TPI in 2020; (f), high (>0.8) TPI in 2020).

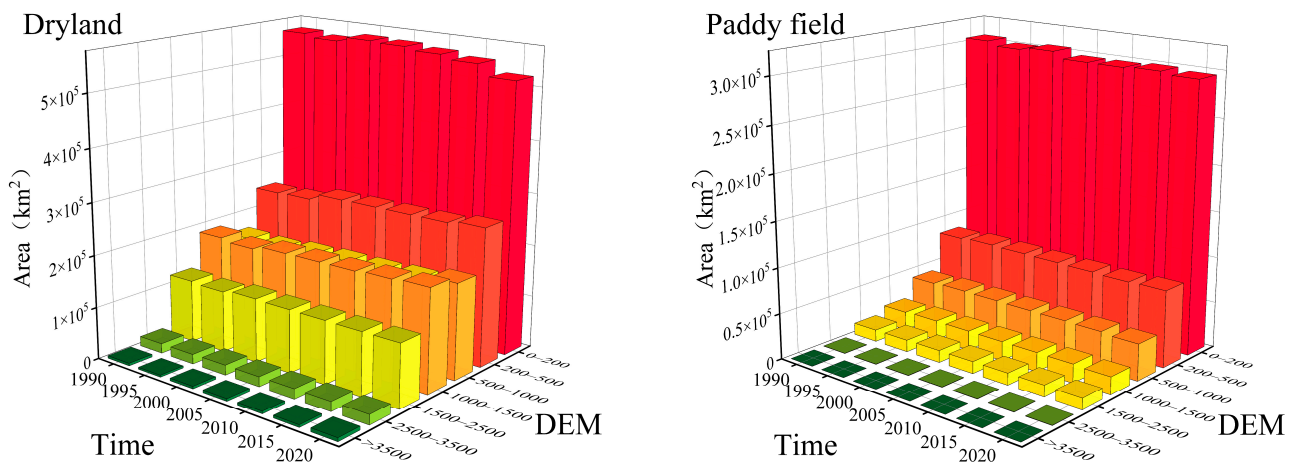


**Figure 2.** Changes in the elevations of paddy field and dryland. (For detailed data, refer to Table S2 in the Supplementary Materials).

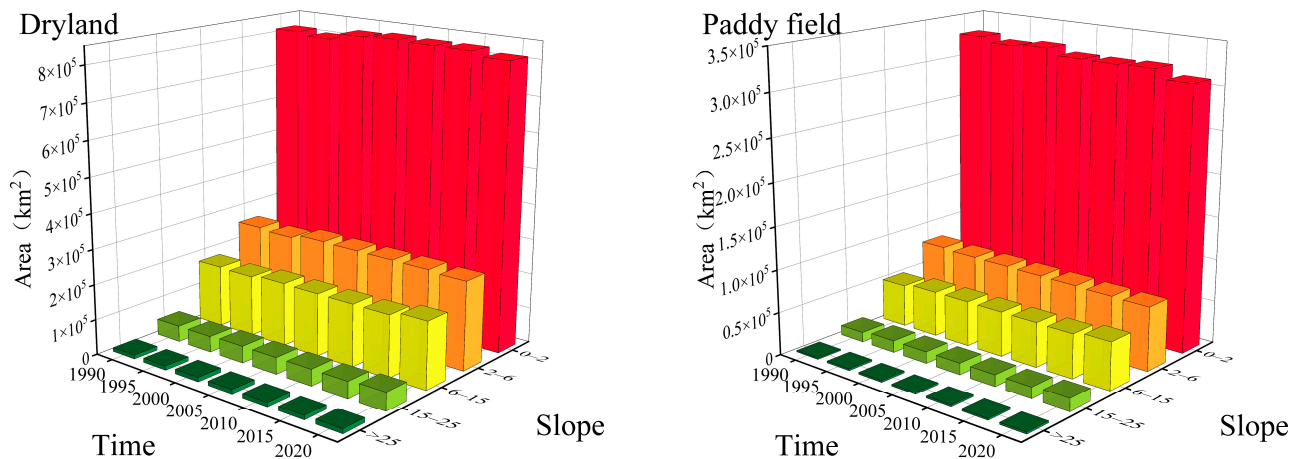


**Figure 3.** Change in the slopes of paddy field and dryland. (For detailed data, refer to Table S3 in the Supplementary Materials).

When looking at the slope aspects (Figure 4), the results showed that the paddy fields and drylands were mainly distributed on the southern, southwestern, southeastern, eastern, and western slopes of hills or mountains. Moreover, important to note is that the area of paddy fields and drylands on southeastern, southern, and southwestern slopes generally decreased, while the area of paddy fields and drylands on northwestern, northern, and northeastern slopes generally increased. Moreover, the area of paddy fields and drylands increased the most in the north, whereas the area of paddy fields decreased most in the south, and drylands decreased most in the southeast. The results indicate that the area of paddy fields and drylands with better light conditions decreased. Under the influence of man-made disturbance in the urbanization process, the advantages of ideal light and heat resources on arable land were ignored, and the area of paddy fields and drylands with superior natural conditions were reduced.

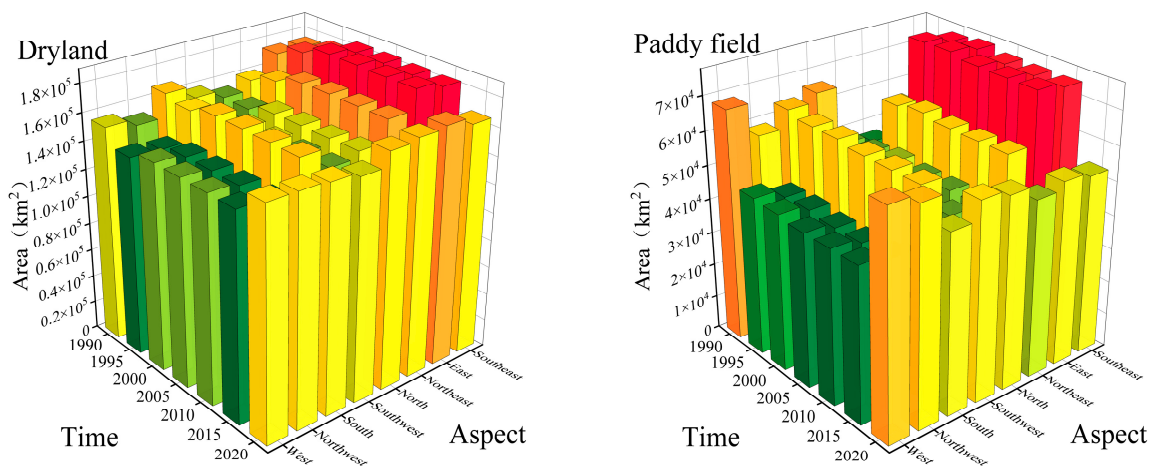


**Figure 4.** Change in the slope aspects of paddy field and dryland. (For detailed data, refer to Table S4 in the Supplementary Materials).

### 3.2. The Land Conversion of Paddy Field, Dryland, and Other Land

The spatial distribution of the land-use changes among paddy field, dryland, and other land from 1990 to 2020 is shown in Figure 5.

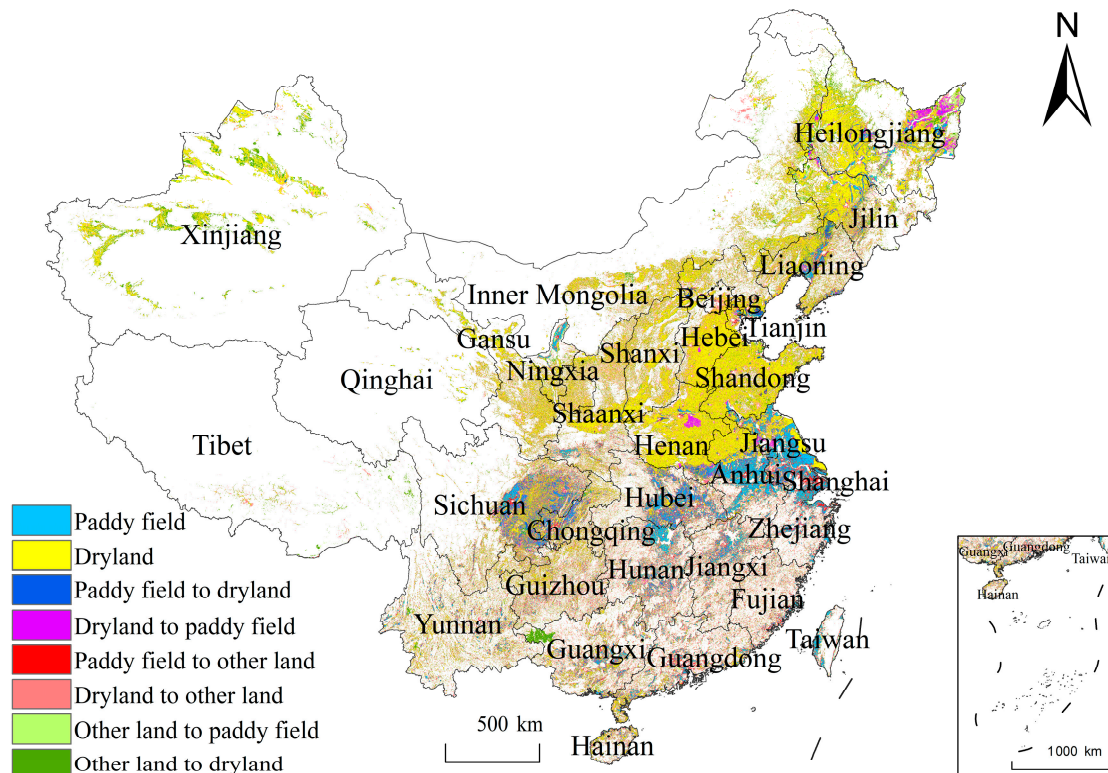


**Figure 5.** Land conversion between paddy field, dryland, and other land from 1990 to 2020.

In terms of the loss of paddy fields, the transition from paddy field to dryland was concentrated in Sichuan, Hebei, and Liaoning provinces. The seasonal water shortage and the decline in groundwater levels may be the major reasons for this change. On the North China Plain, long-term planting and industrial production induces severe groundwater shortages, which form a huge groundwater “funnel” in China. To reduce massive water usage, the government is actively encouraging farmers to change paddy field to dryland by providing subsidies [25]. In Sichuan, seasonal drought occurs frequently due to the spatial-temporal variability of rainfall. Eighty percent of the rainfall in Sichuan is concentrated

in May to September. In spring and canicular days, the possibility of droughts is higher than 60% [26]. The transition from paddy field to other land was mostly concentrated in areas with higher urbanization levels, such as the Yangtze River Delta, the Pearl River Delta, and Chengdu–Chongqing. Taking the Yangtze River Delta as an example, fertile land and a temperate climate are beneficial for agricultural production. As one of the richest regions, the Yangtze River Delta contributes more than 20% GDP yearly to the whole country. However, most construction land is transformed from paddy field in this area [27]. Thus, a spatial overlap can be seen between the high-quality paddy fields and economically developed areas [5,9]. As a result, massive losses of paddy fields with better hydrothermal conditions should be protected against with stronger practices, especially in rapidly urbanized areas.

In terms of newly added paddy fields, most of the new paddy fields in the north came from the old drylands, especially in central Henan Province, central Jiangsu Province, and eastern Heilongjiang Province (Table S5 in the Supplementary Materials). In Henan Province, as the hub of the ecological protection and high-quality development strategy of the Yellow River Basin and the Mid-Line of the South–North Water Diversion Project [28], the local paddy field had a good geographical advantage, which helped supply water resources and plain farming and provided the basis for the transition from dryland to paddy fields. In Jiangsu Province, local land consolidation planning policies encouraged the change from dryland plantations to a rice–wheat rotation to increase the economic value of arable land output. This kind of policy support provided a strong incentive for transitioning from local dryland to paddy field. In eastern Heilongjiang Province, the long-term conservation of massive amounts of fertile black soil on the plain area and the flood control projects for rice fields provided sufficient advantages for the transition from dryland to paddy field. Moreover, the consolidation projects of low-yield fields helped to improve the centralization of paddy field patches. In general, paddy field has higher economic benefits (for instance, rice has a higher price compared to wheat and corn), which stimulates farmers to change their dryland to paddy field to obtain a higher income. Because paddy field is a non-negligible source of carbon emissions [29], the transition from dryland to paddy field may lead to an increase in greenhouse gas emissions, which needs further monitoring in future research.

In terms of drylands loss, the transition from dryland to paddy field was concentrated in the central part of Henan Province, the central part of Jiangsu Province, and the eastern part of Heilongjiang Province. The transition from dryland to other land was mainly concentrated in the periphery of urban agglomerations such as the Beijing–Tianjin–Hebei Region. It can be seen that the larger-scale reduced dryland was concentrated in zones with a better natural resource endowment and a stronger economic location.

In terms of the newly added drylands, the transition from paddy field to dryland was concentrated in Sichuan, Hebei, and Liaoning, and a larger scale of converting other land to dryland was more concentrated in Xinjiang and Guangxi. Among them, converting other land to dryland in Guangxi was mainly concentrated in the west of Guangxi, and the primary source of new, local dryland was the reclamation of abandoned industrial and mining land. The new dryland came from areas with poor suitability for development and utilization.

### 3.3. Land-Type Change in Paddy Field and Dryland under Different Topographic Conditions

#### 3.3.1. Land-Type Change in Paddy Field and Dryland at Different Elevations

Land conversion between paddy field, dryland, and other land from 1990 to 2020 was mainly concentrated at an elevation of 0–200 m (Figure 6). Among them, the greatest area of land conversion occurred between dryland and other land, followed by the conversion between paddy field and other land. The area of the conversion between paddy field and dryland was the lowest.

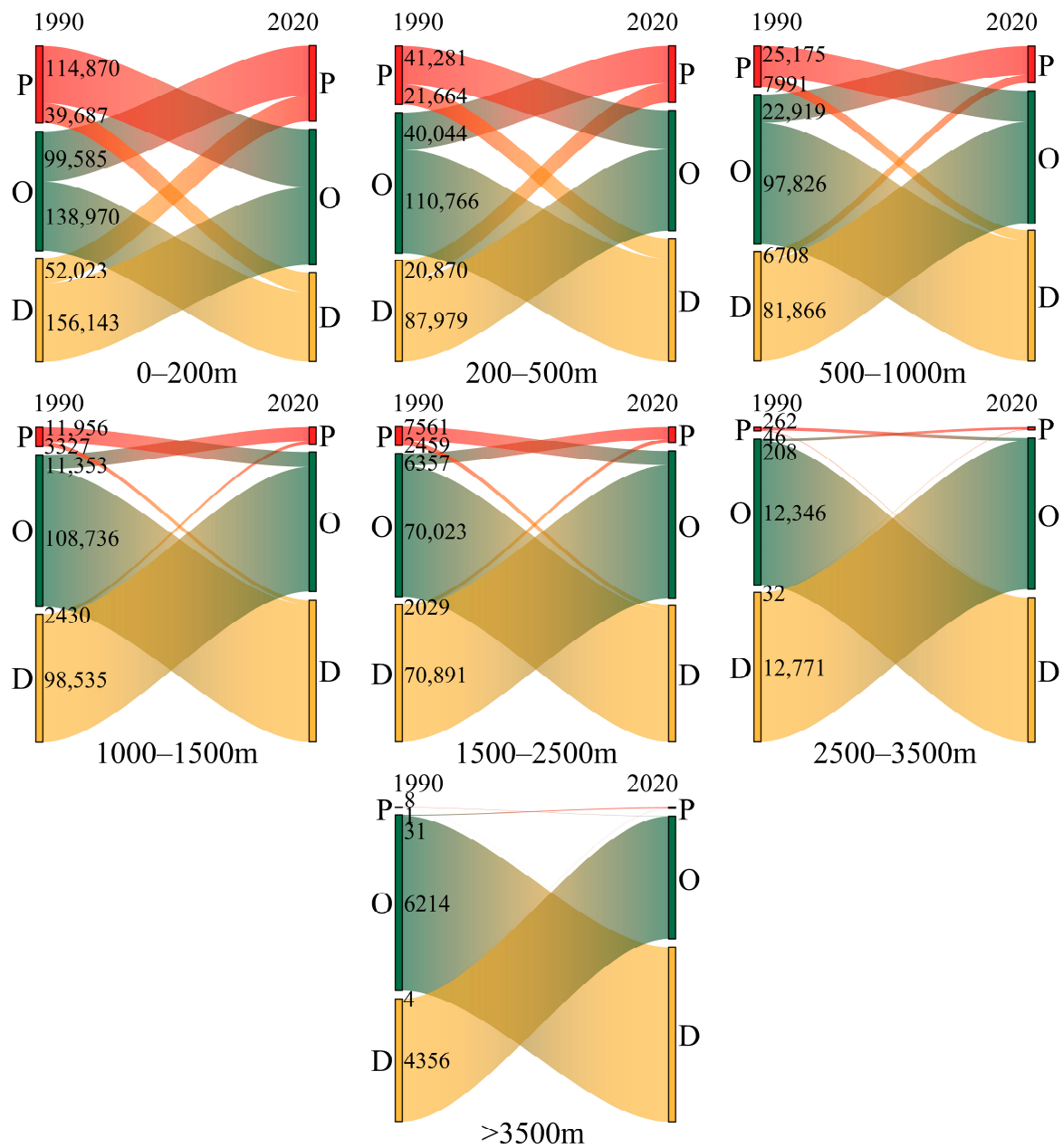


**Figure 6.** Land conversion between paddy field, dry land, and other land at different elevations from 1990 to 2020. P, paddy field; D, dryland; O, other land. The numbers in the figures refer to the area among the land changes (km<sup>2</sup>).

It is worth noting that when looking at the interconversion between paddy field and dryland, the results show that at a 0–200 m elevation, the area changed from dryland to paddy field was much greater than that of paddy field to dryland. On the contrary, at a >200 elevation, the change from paddy field to dryland was more than that of dryland to paddy field.

In terms of the conversion between paddy field and other land, the area of paddy field to other land at each elevation was more than that of other land to paddy field. Unlike paddy field, the conversion between dryland and other land was not only active at the 0–200 m elevation but also significant at the 1000–1500 m elevation (the “second ladder” of China). This discovery confirms the importance of further analyzing the change in dryland and other lands at higher elevations in western China.

### 3.3.2. Land-Type Change in Paddy Field and Dryland at Different Slopes

From 1990 to 2020, land conversion among paddy field, dryland, and other land was mainly located on 0–2° slopes, and the area of land-use change decreased along with the increase in slope (Figure 7). Among them, the land conversion area between dryland and other land was the largest, followed by the conversion between paddy field and other land, whereas the conversion between paddy field and dryland was the lowest. In terms of the interconversion between paddy field and dryland, the area changed from dryland to paddy field at a 0–2° slope was more than that of paddy field to dryland, but on other slopes, the area changed from paddy field to dryland was larger. In terms of the conversion between dryland and other land, the dryland area changed to other land on a >25° slope was more than that of other land to dryland, but on other slopes, the area changed from other land to dryland was higher. In terms of the conversion between paddy field and other land, the area changed from paddy field to other land was more than that of other land to paddy field on slopes, which indicates that the decrease in the paddy field area was significant whether the terrain conditions were steep or flat.

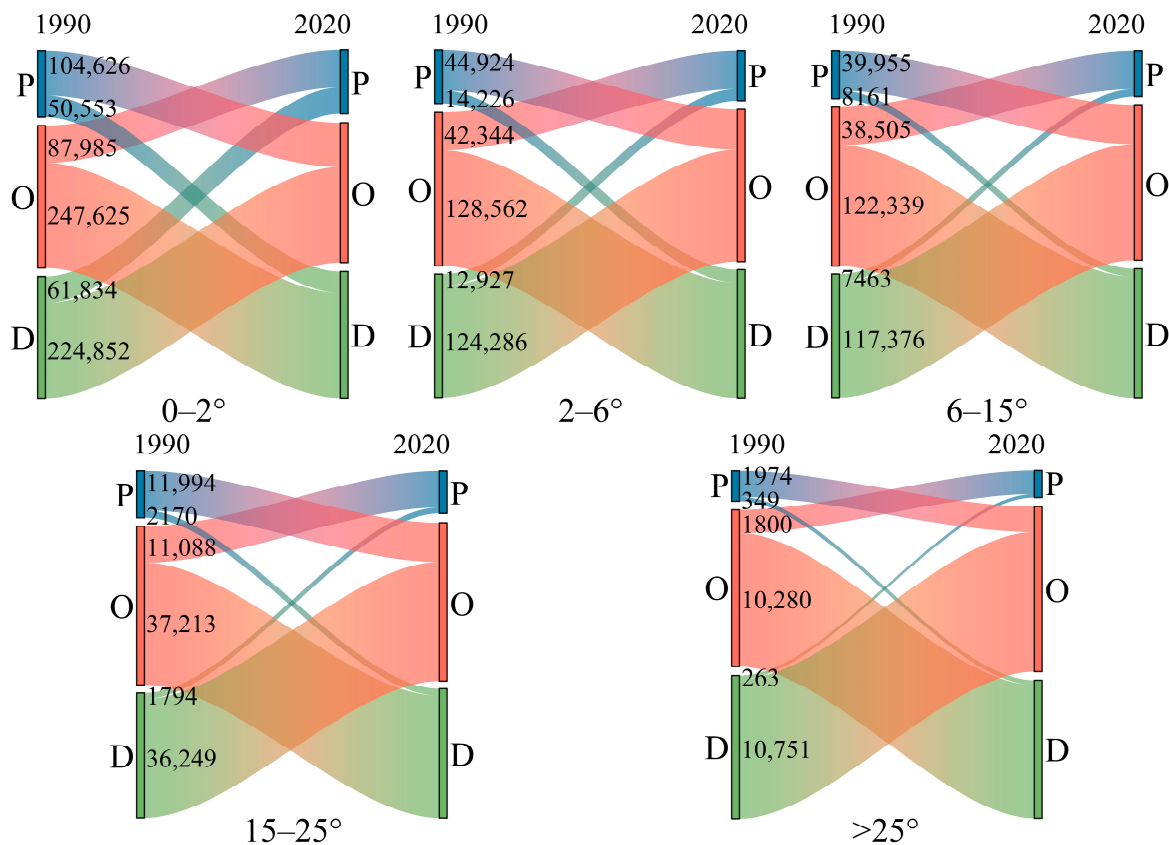


**Figure 7.** Land conversion between paddy field, dryland, and other land at different slopes from 1990 to 2020.

### 3.3.3. Land-Type Change in Paddy Field and Dryland on Different Slope Aspects

On the eastern slope, the conversion from paddy field to dryland, the conversion from dryland to other land, and the conversion from paddy field to other land were the largest. On the western slope, the change from dryland to paddy field, the change from other land to dryland, and the change from other land to paddy field were the greatest.

The conversion between dryland and other land was the most prominent, the conversion between paddy field and other land was the second-most prominent, and the conversion between paddy field and dryland was the least prominent.

It is worth noting that, when comparing the southern slope (with better photothermal conditions) and the northern slope (with worse light conditions), the results show that the

loss of paddy field and dryland was greater on the southern slope than on the northern slope, while the increase in paddy field and dryland was greater on the northern slope than on the southern slope. In other words, the paddy fields and drylands with better light conditions in mountainous and hilly areas decreased (Figure 8).

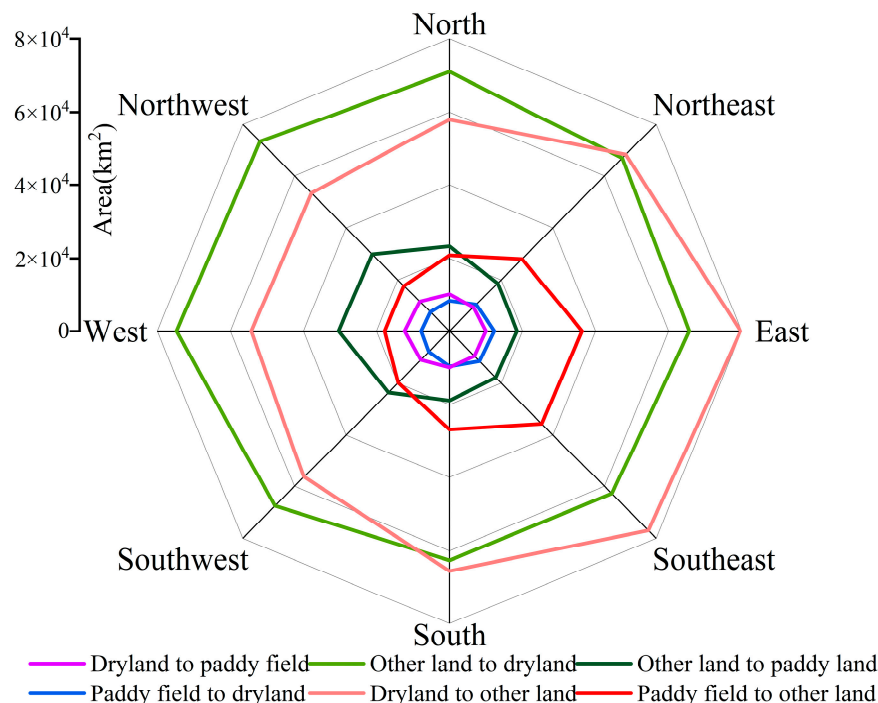


**Figure 8.** Land conversion between paddy field, dryland, and other land at different slope aspects from 1990 to 2020.

### 3.4. The Landscape Characteristics of Paddy Field and Dryland under Different Topographic Conditions

The landscape indexes of paddy field from 1990 to 2020 are shown in Table 3. In terms of the intensity indices, the NP and PD increased, which indicates that the landscape of the paddy field became more fragmented. The LPI increased, which indicates that the dominance of the main paddy field patches increased. Specifically (Tables S6–S8 in the Supplementary Materials), the largest NPs appeared at 200–500 m, on a 2–6° slope, and on the western slope aspect; the largest increase in the NP appeared at 200–500 m, on a 15–25° slope, and on the northern slope aspect; the largest decrease in the NP appeared at 0–200 m, on a 2–6° slope, and on the southern slope aspect. The largest PDs were distributed at 2500–3500 m, on a 15–25° slope, and on the northeastern slope aspect. The largest increase in the PD appeared at >3500 m and on the southern slope aspect, and the largest decrease in the PD appeared on a 6–15° slope and the northwestern slope aspect. The largest LPIs were distributed at >3500 m DEM, on a 0–2° slope, and on the southeastern slope aspect; the largest increase in the LPI was distributed at 0–200 m and on the southern slope aspect; the largest decrease in the LPI was distributed at >3500 m, on a 6–15° slope, and on the southeastern slope aspect.

In terms of the shape indices, the AWMSI and LSI experienced fluctuated growth, which indicates that the shape of the paddy patches tended to be complex and irregular. Specifically (Tables S6–S8 in the Supplementary Materials), the largest LSIs were distributed at 0–200 m, on a 2–6° slope, and on the western slope aspect; the largest increase in the LSI appeared at 200–500 m, on a 15–25° slope, and on the northern slope aspect; the largest decrease in the LSI appeared at 0–200 m, on a 2–6° slope, and on the southern slope aspect. The largest AWMSIs were distributed at 0–200 m, on a 0–2° slope, and on the southeastern slope aspect; the largest increase in the AWMSI was distributed at 0–200 m;

the largest decrease in the AWMSI was distributed at 200–500 m, on a 0–2° slope, and on the southeastern slope aspect.

In terms of the vergence indices, the AI decreased while the DIVISION and SPLIT increased, which meant that the landscape of paddy field tended to be more dispersed. Specifically (Tables S6–S8 in the Supplementary Materials), DIVISION decreased at 0–200 m and 1000–1500 m but increased at other elevations, slopes, and slope aspects. The largest SPLITS were distributed at 200–500 m, on a 2–6° slope, and on the western slope aspect, whereas the largest increase in the number of SPLIT was distributed at 200–500 m, on a 6–15° slope, and on the northern slope aspect, and the largest decrease in the number of SPLIT was distributed at 1000–1500 m, on a 2–6° slope, and on the southern slope aspect. The largest AIs were distributed at 0–200 m, on a 0–2° slope, and on the western slope aspect, the largest increase in the AI was distributed on a >25° slope and on the northwestern slope aspect, and the largest decrease in the number of SPLIT was distributed at >3500 m, on a 0–2° slope, and on the southern slope aspect. After 2015, the AI increased while the DIVISION and SPLIT decreased slightly, which indicates that along with the land consolidation projects, the landscape of paddy field appeared to be more concentrated.

**Table 3.** Results of the landscape pattern analysis of paddy field.

Category	Index	1990	1995	2000	2005	2010	2015	2020
Intensity	NP	63,269	62,748	63,935	64,902	65,098	65,753	64,574
	PD	0.1339	0.1331	0.1349	0.1393	0.14	0.1414	0.1405
	LPI	12.55	12.23	13.65	13.80	13.70	13.46	14.23
Shape	LSI	334.23	334.05	337.28	340.51	342.46	345.18	337.89
	AWMSI	14.85	15.00	16.03	15.93	15.93	15.65	16.05
Vergence	AI	51.44	51.39	51.06	50.15	49.85	49.44	50.23
	DIVISION	0.9775	0.9789	0.9762	0.9763	0.977	0.978	0.9776
	SPLIT	44.35	47.34	42.08	42.25	43.41	45.38	44.52

The intensity indices of dryland are shown in Table 4. The NP and PD increased while the LPI decreased, which indicates that the landscape fragmentation of dryland became more significant. Specifically (Tables S9–S11 in the Supplementary Materials), the largest NPs were distributed at 500–1000 m, on a 2–6° slope, and on the eastern slope aspect; the largest increase in the NP appeared at 500–1000 m, on a 6–15° slope, and on the northern slope aspect; the largest decrease in the NP appeared at 0–200 m, on a 0–2° slope, and on the southeastern slope aspect. The largest PDs were distributed at >3500 m, on a >25° slope, and on the western slope aspect; the largest increase in the PD was distributed at 1500–2500 m and on the eastern slope aspect; the largest increase in the PD was distributed at >3500 m, on a 15–25° slope, and on the northern slope aspect. The largest LPIs were distributed at 0–200 m, on a 0–2° slope, and on the northern slope aspect; the largest increase in the number of LPIs was distributed at 0–200 m, on a 6–15° slope, and on the northern slope aspect; the largest decrease in the number of LPIs was distributed at >3500 m, on a 0–2° slope, and on the southern slope aspect.

In terms of the shape indices, the AWMSI and LSI increased, which indicates that the shape of the dryland tended to be more complex and irregular. Specifically (Tables S9–S11 in the Supplementary Materials), the largest LSIs were distributed at 1000–1500 m, on a 2–6° slope, and on the eastern slope aspect; the largest increase in the LSI was distributed at 500–1000 m, on a 15–25° slope, and on the northern slope aspect; the largest decrease in the LSI was distributed at 1000–1500 m, on a 2–6° slope, and on the southeastern slope aspect. The largest AWMSIs were distributed at 0–200 m, on a 0–2° slope, and on the northern slope aspect; the largest increase in AWMSI was distributed at 0–200 m, on a 0–2° slope, and on the northern slope aspect; the largest decrease in the AWMSI was distributed at 1000–1500 m, on a 2–6° slope, and on the southern slope aspect.

In terms of the vergence indices, the AI decreased while the DIVISION and SPLIT increased, which proves the fragmentation and diversification characteristics of dryland

landscape. Specifically (Tables S9–S11 in the Supplementary Materials), DIVISION was larger at other elevations, slopes, and slope aspects; the largest increase in the DIVISION was distributed at >3500 m, on a 0–2° slope. The largest SPLITs were distributed at 2500–3500 m, on a 15–25° slope, and on the western slope aspect; the most significant increase in SPLIT was distributed at >3500 m, on a >25° slope, and on the western slope aspect; the largest decrease in the SPLIT was distributed at 200–500 m, on a 6–15° slope, and on the northern slope aspect. The largest AIs was distributed at 0–200 m, on a 0–2° slope, and on the northern slope aspect.

**Table 4.** Results of the landscape pattern analysis of dryland.

Category	Index	1990	1995	2000	2005	2010	2015	2020
Intensity	NP	107,926	105,567	108,719	109,163	109,796	111,141	110,920
	PD	0.0831	0.0822	0.082	0.0822	0.083	0.0841	0.0839
	LPI	30.69	25.04	28.64	27.98	27.90	27.02	25.19
Shape	LSI	455.79	448.42	459.63	460.44	462.10	466.72	464.46
	AWMSI	56.50	51.63	59.65	57.21	57.12	56.80	57.27
Vergence	AI	60.06	60.46	60.13	60.07	59.86	59.44	59.65
	DIVISION	0.8988	0.9256	0.9073	0.9126	0.9132	0.9166	0.9163
	SPLIT	9.89	13.44	10.78	11.45	11.52	11.99	11.94

In general, the landscape fragmentation of paddy field and dryland increased, but dryland showed a higher aggregate degree and more obvious change towards complex shapes and fragmentation of land plots. Furthermore, most of the fragmentation and complexity in the shape of paddy field and dryland were concentrated in low-elevation areas with flat terrain, which emphasizes the loss of high-quality arable land with superior topographic conditions. In addition, the dryland in high-elevation areas tended to be more dispersed and more complicated, which needs further observation for long-term agricultural production.

#### 4. Discussion

##### 4.1. Changes in Microterrain Factors Led to a Decrease in Paddy Field and Dryland with Good Photothermal Conditions

As the primary resources of arable land use, water, heat, light, and other natural factors impact the growth of crops. Scholars have found that as a microterrain factor, the slope aspect has a significant effect on the growth and spatial distribution of plants [30]. The slope aspect determines the photothermal conditions of vegetation through the reception of solar radiation and hydrological processes which, in turn, affects crop growth. In countries in the Northern Hemisphere, the northern slope aspect has lower temperatures, lower light intensity, higher relative humidity, and more abundant soil nutrients [31–33], while the southern slope aspect has sufficient light, less moisture, and large diurnal temperature differences. Therefore, most studies indicate that plants on the southern slope aspect have a higher photosynthetic level and are more productive [34–36]. Similarly, this paper showed that 40.56% of paddy fields and 38.48% of drylands in China were distributed on the southern, southwestern, and southeastern slope aspects, which further proves the higher suitability of paddy field and dryland use on southern slopes.

However, the results of this paper found that the area of paddy field and dryland with better light conditions in China was decreasing. The area of paddy fields and drylands on the southeastern, southern, and southwestern slopes generally decreased from 1990 to 2020 but increased on the northwestern, northern, and northeastern slopes. Furthermore, conversion from paddy field and dryland to other land was more active on the southern, southeastern, eastern, and northeastern slopes. These results indicate the worsened solar-thermal conditions of paddy field and dryland, which may cause an explicit potential decline in the productivity of arable land. Though some studies have paid attention to the change in arable land area and spatial distribution, the change in productivity caused by

the microterrain changes in arable land is rarely discussed, which needs further attention in future research.

#### *4.2. In Addition to the “Third Ladder”, the Changes in Paddy Field and Dryland Have Become Active on the “Second Ladder” of China*

The terrain of China is high in the west and low in the east. According to the elevation from west to east, the whole country can be roughly divided by three ladders including the first ladder (>4000 m) in the west, the second ladder (1000–2000 m) in the middle, and the third ladder (<500 m) in the east. This study found that the land conversion of paddy field and dryland in China mainly occurred in the eastern plain on the third ladder. Similarly, relative studies have supported this conclusion such as the large-scale conversion from paddy field to dryland and construction land in the Beijing–Tianjin–Hebei Region [37], the conversion from other land to dryland and paddy field in the Northeast China Plain [4,15], and the conversion from paddy field and dryland to construction land in Yangtze Plain areas [27].

It is worth emphasizing that this article has a new finding. In addition to the third ladder, the transition between paddy field, dryland, and other land on the second ladder was also active (such as at an elevation of 1000–1500 m). Coincidentally, Chi [38] and Dong [39] also found that a large area of the land conversion of paddy field, dryland, and other land occurred on the second ladder, such as Inner Mongolia, in recent years. Therefore, the land-use change in paddy field and dryland became active on the second ladder. Although climatic conditions, population density, and economic development on the second ladder are poorer than that on the third ladder, the use of arable land at higher elevations is proven to have increased.

The reasons for this can be found by tracing the regional development of the second ladder. Since the implementation of the China Western Development Strategy in 2000, the Chinese government has increased its support for land consolidation and basic arable land construction in the west and has carried out a series of ecological restoration projects to prevent desertification and improve the ecological environment of arable land. Such policy supports resulted in a significant increase in new agricultural modernization, agricultural capital investment, and per capita arable land area [40]. After the agricultural tax was abolished by the No. 1 Central Document in 2006, “The Guidance on Promoting Sustainable Development of Agriculture and Animal Husbandry in Northwest Arid Regions” was issued, which increased agricultural subsidies in poor areas in West China. These have further motivated the enthusiasm for farm production on the second ladder.

It is worth mentioning that in 2017, the government began to permit trans-provincial “land-ticket transactions” to keep an arable land requisition–compensation balance (i.e., arable land occupied by urban construction in provinces with a land shortage can be replenished by provinces with abundant arable land reserve resources). Benefited by abundant land resources, the provinces on the second ladder developed and replenished a large amount of new arable land in “land-ticket transactions”, which has also contributed to the dramatic land conversion between paddy field, dryland, and other land at the second ladder.

However, because of the special arid climate environment of the second ladder, the increase in arable land in this area may further intensify the contradiction of water use [41], which will cause the degradation of the ecosystem and the quality of arable land and lead to an increase in desertification over the long term [42–44]. Therefore, faced with the active conversion of paddy field and dryland on the second ladder, the local government needs to focus on pushing forward the delineation of the “three lines” (i.e., urban development boundary, permanent basic arable land, and ecological protection red line) and the “three areas” (i.e., urban space, agricultural space, and ecological space) in territorial space planning. Unsuitable arable land with high costs and ecological risks should be retired and the reclamation of arable land in ecologically fragile areas should be limited to rationalize the land-use structure at a higher elevation. Moreover, large-scale land use in Europe has

shown some adverse effects such as the persistence of pesticides and other agricultural inputs. Taking a cue from this, the government in China has new opportunities and challenges [45]. The government should further strengthen the arable land-use intensity and high-standard cropland construction and actively promote the protection of arable land such as by letting land lie fallow and through reasonable crop rotation [46]. To improve the acceptance of environmentally friendly techniques, the government should provide more subsidies for eco-friendly agriculture to farmers.

#### *4.3. Increased Paddy Field and Dryland on Slopes Exacerbated the Erosion Risk*

From the perspective of land suitability, arable land in low-elevation plains is rich in water and heat resources, which is more suitable for agricultural production. This study found that paddy fields at low elevations (0–200 m) accounted for 64.6% of the total paddy field area, and paddy fields on low slope (0–2°) areas accounted for 67.62% of the total paddy field area. Drylands at low elevations (0–200 m) and low slopes (0–2°) accounted for 39.78% and 61.46% of the total dryland area, respectively. Compared with dryland, paddy field is more sensitive to topography and have higher requirements for water retention. However, this study found that the paddy field and dryland went “up the hill”, i.e., an increasing number of paddy fields and drylands appeared at higher elevations (>200 m) and steeper slopes (>6°). Because of the large quick water flow on slopes, the phenomenon of soil and water erosion caused by the increase in paddy field and dryland on slopes needs more attention [47]. Rice cultivation in China and Southeast Asia is an important source of farmers’ income. The increasingly unideal topographic conditions of paddy fields may bring about more socioeconomic uncertainties, which need further study on the consequences by researchers.

In addition, in terraced fields on slopes, paddy fields tend to exhibit a higher water and fertilizer retention capacity and lower soil erosion intensity than drylands [48]. For example, Gao [49] and Xiao [50] found that paddy fields were less affected by soil erosion than drylands in karst areas, and Chen [51] pointed out that the paddy fields in Taiwan’s mountains were less affected by rainfall erosion than drylands. However, this paper found that the transition from paddy field to dryland within a >2° slope and >200 m elevation was greater than the transition from dryland to paddy field. Taking the mountainous southwest China (including Chongqing, Sichuan, Guizhou, and Yunnan) as an example, the area of paddy field to dryland within a >2° slope and >200 m elevation was 24,080 and 25,981 km<sup>2</sup>, respectively, which is much higher than the area from dryland to paddy field (15,022 and 16,561 km<sup>2</sup>). As a result, considering the massive change from paddy field to dryland, stronger water–soil conservation is highly needed to improve the productivity of mountainous arable land.

#### *4.4. The Landscape Fragmentation of Paddy Field and Dryland Emphasize the Importance of Land Consolidation*

This study states that paddy field and dryland both tended to be dispersed, fragmented, and complex in shape, but compared with paddy field, dryland was more aggregated and showed a stronger change towards complex and fragmented shapes.

Similarly, previous studies showed that Heilongjiang had increased fragmentation in terms of the paddy field landscape [14,52]; landscape fragmentation and the heterogeneity of dryland and paddy field were intensified in Guangdong Province [21]. Moreover, the paddy field in the Jinjing River of Hunan [19] and the paddy field and dryland in the Dongting Lake area [22] showed increased fragmentation and dispersed distribution. These findings are consistent with the conclusions of this paper. Inversely, the decrease in landscape fragmentation of dryland in the Horqin region [53], the fluctuating fragmentation of paddy field and dryland in the Loess Plateau [54], and the decline in the fragmentation of dryland and paddy field decreased in the Karst area of Chishui City [55] and Zhoushan Island [56]. These conclusions are partly different in this study. As a result, the landscape characteristics of paddy field and dryland have zonal differences, but both show fragmentation, irregular shape, and complex distribution. Therefore, increasing the concentration

level and contiguity of land plots and strengthening the infrastructure of water, roads, and forests via targeted land consolidation projects should be the major measures used to alleviate the inefficiency of arable land production caused by the unpredictable landscape characteristics of paddy field and dryland.

## 5. Conclusions

Based on 1 km land-use grid data from 1990 to 2020, this study applied a landscape analysis, the land-use change matrix for different topographic grades of China, to determine the divergent patterns and the spatial–temporal changes in paddy field and dryland resources under different terrain gradients. The results show that:

First, although paddy field and dryland were mostly distributed in areas with better photothermal conditions, the area of paddy fields and drylands on sunny slopes significantly decreased in recent years. The area of paddy fields and drylands on the southeastern, southern, and southwestern slopes decreased, while the area of paddy fields and drylands on the northwestern, northern, and northeast slopes increased.

Second, from 1990 to 2020, land conversion between paddy field, dryland, and other land was mainly concentrated in the third ladder (0–200 m DEM), but the changes in the second ladder (500–2500 m DEM) became prominent.

Third, paddy field and dryland went “up the hill”. Paddy field and dryland at low-elevation, low-sloping areas were reduced, and those at higher-elevation, higher-sloping areas increased, which may trigger potential soil erosion. Meanwhile, at high slopes and high elevations, the transition from paddy field to dryland was more prominent.

Finally, there were differences in the landscape characteristics of paddy field and dryland. Although the fragmentation of patches, dispersion of distribution, and complexity of shapes of paddy field landscapes increased, the new paddy field showed the characteristics of aggregation in some areas (such as the northeast and Sichuan). In contrast, although the fragmentation of patches, dispersion of distribution, and complexity of shapes of dryland landscapes increased, the landscape agglomeration characteristics were higher compared to paddy field, decreasing with time.

Based on the research findings, this paper puts forward some suggestions on the utilization of paddy field and dryland. Firstly, the government should strengthen the protection of arable land on sunny slopes and control the conversion from arable land to construction land on sunny slopes in traditional agricultural production areas. Secondly, the protection of water resources in the utilization of arable land in the second ladder regions (such as Xinjiang and Gansu) should be strengthened, and unsuitable arable land should be retired from agricultural production. Thirdly, the government should protect the arable land on the plain area and limit the extensive use of paddy field and dryland on sloping areas to reduce the aggravation of soil erosion. Lastly, land consolidation should emphasize reducing the landscape fragmentation and dispersed distribution of arable land patches.

**Supplementary Materials:** The following supporting information can be downloaded at: <https://www.mdpi.com/article/10.3390/land11101851/s1>. Table S1: The area of paddy field and dryland under different TPI in China in 1990 and 2020; Table S2: Change in the elevations of paddy field and dryland; Table S3: Change in the slopes of paddy field and dryland; Table S4: Change in slope aspects of paddy field and dryland; Table S5: Land use transformation matrices for paddy field, dryland, and other land among the 32 provinces; Table S6: Landscape indices of paddy field in different elevations; Table S7: Landscape indices of paddy field in different slopes; Table S8: Landscape indices of paddy field in different slope aspects; Table S9: Landscape indices of dryland in different elevations; Table S10: Landscape indices of dryland in different slopes; Table S11: Landscape indices of dryland in different slope aspects.

**Author Contributions:** Conceptualization, S.X.; methodology, S.X.; software, S.X.; formal analysis, S.X.; investigation, W.W., Q.S. and Z.Z.; data curation, S.X. and W.W.; writing—original draft preparation, S.X.; writing—review and editing, G.Y.; visualization, S.X.; supervision, G.Y.; project administration, S.X.; funding acquisition, G.Y. All authors have read and agreed to the published version of the manuscript.

**Funding:** This paper was funded by the National Natural Science Foundation of China (Project No. 42171253); the Humanities and Social Sciences Foundation of Shandong Province, China (Project No. 2021-JCGL-08); the Shandong Social Science Planning Fund Program (Project No. 21CCXJ15); the Youth Innovation Team of Shandong Universities, China—“The Youth Innovation Science and Technology Support Program” (Project No. 2021RW034); the Research Project of Teaching Reform of Shandong Normal University (2019XM42).

**Data Availability Statement:** Data are available in a publicly accessible repository that does not issue DOIs. Publicly available data sets were analyzed in this study. These data can be found here: <https://www.resdc.cn/>, accessed on 10 February 2021.

**Acknowledgments:** The authors extend great gratitude to the anonymous reviewers and editors for their helpful review and critical comments. We confirm all individuals consent.

**Conflicts of Interest:** The authors declare no conflict of interest.

## References

- Ning, J.; Liu, J.; Kuang, W. Spatiotemporal patterns and characteristics of land-use change in China during 2010–2015. *J. Geogr. Sci.* **2018**, *28*, 547–562. [[CrossRef](#)]
- Zhou, Y.; Li, Y.; Xu, C. Land consolidation and rural revitalization in China: Mechanisms and paths. *Land Use Pol.* **2020**, *91*, 104379. [[CrossRef](#)]
- Zhou, Y.; Li, X.; Liu, Y. Cultivated land protection and rational use in China. *Land Use Pol.* **2021**, *106*, 105454. [[CrossRef](#)]
- Liu, Y.; Liu, X.; Liu, Z. Effects of climate change on paddy expansion and potential adaption strategies for sustainable agriculture development across Northeast China. *Appl. Geogr.* **2022**, *141*, 102667. [[CrossRef](#)]
- Cheng, C.; Yang, X.; Cai, H. Analysis of Spatial and Temporal Changes and Expansion Patterns in Mainland Chinese Urban Land between 1995 and 2015. *Remote Sens.* **2021**, *13*, 2090. [[CrossRef](#)]
- Xu, X.; Wang, L.; Cai, H. The influences of spatiotemporal change of cultivated land on food crop production potential in China. *Food Secur.* **2017**, *9*, 485–495. [[CrossRef](#)]
- Lou, Y.; Yin, G.; Xin, Y. Recessive Transition Mechanism of Arable Land Use Based on the Perspective of Coupling Coordination of Input-Output: A Case Study of 31 Provinces in China. *Land* **2021**, *10*, 41. [[CrossRef](#)]
- Yin, G.; Jiang, X.; Xin, Y. Dilemma and solution of land scarcity, agro-production, and environmental risk for typical grain-producing areas in rapid urbanizing process in China. *Environ. Sci. Pollut. Res.* **2021**, *28*, 28606–28623. [[CrossRef](#)]
- Li, T.; Long, H.; Zhang, Y. Analysis of the spatial mismatch of grain production and farmland resources in China based on the potential crop rotation system. *Land Use Pol.* **2017**, *60*, 26–36. [[CrossRef](#)]
- Wang, Q.; Li, Y.; Luo, G. Spatiotemporal change characteristics and driving mechanism of slope cultivated land transition in karst trough valley area of Guizhou Province, China. *Environ. Earth Sci.* **2020**, *79*, 284. [[CrossRef](#)]
- Jiang, S.; Chen, X.; Smettem, K. Climate and land use influences on changing spatiotemporal patterns of mountain vegetation cover in southwest China. *Ecol. Indic.* **2021**, *121*, 107193. [[CrossRef](#)]
- Shi, F.; Liu, S.; Sun, Y. Ecological network construction of the heterogeneous agro-pastoral areas in the upper Yellow River basin. *Agric. Ecosyst. Environ.* **2020**, *302*, 107069. [[CrossRef](#)]
- Gong, Y.; Li, J.; Li, Y. Spatiotemporal characteristics and driving mechanisms of arable land in the Beijing-Tianjin-Hebei region during 1990–2015. *Socio-Econ. Plan. Sci.* **2020**, *70*, 100720. [[CrossRef](#)]
- Li, D.; He, L.; Qu, J. Spatial evolution of cultivated land in the Heilongjiang Province in China from 1980 to 2015. *Environ. Monit. Assess.* **2022**, *194*, 444. [[CrossRef](#)] [[PubMed](#)]
- Chen, L.; Zhao, H.; Song, G. Optimization of cultivated land pattern for achieving cultivated land system security: A case study in Heilongjiang Province, China. *Land Use Pol.* **2021**, *108*, 105589. [[CrossRef](#)]
- Gao, X.; Cheng, W.; Wang, N. Spatio-temporal distribution and transformation of cropland in geomorphologic regions of China during 1990–2015. *J. Geogr. Sci.* **2019**, *29*, 180–196. [[CrossRef](#)]
- Li, J.; Li, Z.; Lü, Z. Analysis of spatiotemporal variations in land use on the Loess Plateau of China during 1986–2010. *Environ. Earth Sci.* **2016**, *75*, 997. [[CrossRef](#)]
- Zhao, Y.; Tomita, M.; Hara, K. Effects of topography on status and changes in land-cover patterns, Chongqing City, China. *Landsc. Ecol. Eng.* **2014**, *10*, 125–135. [[CrossRef](#)]
- Liu, X.; Li, Y.; Shen, J. Landscape pattern changes at a catchment scale: A case study in the upper Jinjing river catchment in subtropical central China from 1933 to 2005. *Landsc. Ecol. Eng.* **2014**, *10*, 263–276. [[CrossRef](#)]
- Zhong, T.; Huang, X.; Zhang, X. Temporal and spatial variability of agricultural land loss in relation to policy and accessibility in a low hilly region of southeast China. *Land Use Pol.* **2011**, *28*, 762–769. [[CrossRef](#)]
- Liu, L.; Liu, Z.; Gong, J. Quantifying the amount, heterogeneity, and pattern of farmland: Implications for China’s requisition-compensation balance of farmland policy. *Land Use Pol.* **2019**, *81*, 256–266. [[CrossRef](#)]

22. Yin, G.; Liu, L.; Jiang, X. The sustainable arable land use pattern under the tradeoff of agricultural production, economic development, and ecological protection—An analysis of Dongting Lake basin, China. *Environ. Sci. Pollut. Res.* **2017**, *24*, 25329–25345. [[CrossRef](#)] [[PubMed](#)]
23. Shi, Z.; Ma, L.; Zhang, W. Differentiation and correlation of spatial pattern and multifunction in rural settlements considering topographic gradients: Evidence from Loess Hilly Region, China. *J. Environ. Manag.* **2022**, *315*, 115127. [[CrossRef](#)] [[PubMed](#)]
24. Song, W.; Pijanowski, B. The effects of China's cultivated land balance program on potential land productivity at a national scale. *Appl. Geogr.* **2014**, *46*, 158–170. [[CrossRef](#)]
25. Liu, M.; Yang, L.; Min, Q. Eco-compensation standards for agricultural water conservation: A case study of the paddy land-to-dry land program in China. *Agric. Water Manag.* **2018**, *204*, 192–197. [[CrossRef](#)]
26. Zhang, W.; Wei, C.; Zhou, J. Optimal Allocation of Rainfall in the Sichuan Basin, Southwest China. *Water Resour. Manag.* **2010**, *24*, 4529–4549. [[CrossRef](#)]
27. Liu, Y.; Wang, J.; Long, H. Analysis of arable land loss and its impact on rural sustainability in Southern Jiangsu Province of China. *J. Environ. Manag.* **2010**, *91*, 646–653. [[CrossRef](#)]
28. Chen, M.; Bai, Z.; Wang, Q. Habitat Quality Effect and Driving Mechanism of Land Use Transitions: A Case Study of Henan Water Source Area of the Middle Route of the South-to-North Water Transfer Project. *Land* **2021**, *10*, 796. [[CrossRef](#)]
29. Chen, Y.; Chen, X.; Zheng, P. Value compensation of net carbon sequestration alleviates the trend of abandoned farmland: A quantification of paddy field system in China based on perspectives of grain security and carbon neutrality. *Ecol. Indic.* **2022**, *138*, 108815. [[CrossRef](#)]
30. Zheng, C.; Liu, Z.; Fang, J. Tree species diversity along altitudinal gradient on southeastern and northwestern slopes of Mt. Huanggang, Wuyi Mountains, Fujian, China. *Biodivers. Sci.* **2004**, *12*, 63–74.
31. Zhang, W.; Jiang, Y.; Wang, M. Topography- and Species-Dependent Climatic Responses in Radial Growth of *Picea meyeri* and *Larix principis-rupprechtii* in the Luyashan Mountains of North-Central China. *Forests* **2015**, *6*, 116–132. [[CrossRef](#)]
32. Yang, J.; El-Kassaby, Y.; Guan, W. The effect of slope aspect on vegetation attributes in a mountainous dry valley, Southwest China. *Sci. Rep.* **2020**, *10*, 16465. [[CrossRef](#)] [[PubMed](#)]
33. Xu, Y.; Zhu, G.; Wan, Q. Effect of terrace construction on soil moisture in rain-fed farming area of Loess Plateau. *J. Hydrol. Reg. Stud.* **2021**, *37*, 100889. [[CrossRef](#)]
34. Fekedulegn, D.; Hicks, R.; Colbert, J. Influence of topographic aspect, precipitation and drought on radial growth of four major tree species in an Appalachian watershed. *For. Ecol. Manag.* **2003**, *177*, 409–425. [[CrossRef](#)]
35. Hishi, T.; Urakawa, R.; Tashiro, N. Seasonality of factors controlling N mineralization rates among slope positions and aspects in cool-temperate deciduous natural forests and larch plantations. *Biol. Fertil. Soils* **2014**, *50*, 343–356. [[CrossRef](#)]
36. Wang, P.; Deng, X.; Jiang, S. Global warming, grain production and its efficiency: Case study of major grain production region. *Ecol. Indic.* **2019**, *105*, 563–570. [[CrossRef](#)]
37. Zhao, S.; Cheng, W.; Liu, H. Land Use Transformation Rule Analysis in Beijing-Tianjin-Tangshan Region Using Remote Sensing and GIS Technology. *J. Sens.* **2016**, *2016*, 6756295. [[CrossRef](#)]
38. Chi, W.; Zhao, Y.; Kuang, W. Impact of Cropland Evolution on Soil Wind Erosion in Inner Mongolia of China. *Land* **2021**, *10*, 583. [[CrossRef](#)]
39. Dong, J.; Liu, J.; Yan, H. Spatio-temporal pattern and rationality of land reclamation and cropland abandonment in mid-eastern Inner Mongolia of China in 1990–2005. *Environ. Monit. Assess.* **2011**, *179*, 137–153. [[CrossRef](#)]
40. Lyu, X.; Wang, Y.; Niu, S. Spatio-Temporal Pattern and Influence Mechanism of Cultivated Land System Resilience: Case from China. *Land* **2022**, *11*, 11. [[CrossRef](#)]
41. Shen, Y.; Li, S.; Chen, Y. Estimation of regional irrigation water requirement and water supply risk in the arid region of Northwestern China 1989–2010. *Agric. Water Manag.* **2013**, *128*, 55–64. [[CrossRef](#)]
42. Zhao, H.; Zhang, F.; Yu, Z. Spatiotemporal variation in soil degradation and economic damage caused by wind erosion in Northwest China. *J. Environ. Manag.* **2022**, *314*, 115121. [[CrossRef](#)] [[PubMed](#)]
43. Jiang, C.; Liu, J.; Zhang, H. China's progress towards sustainable land degradation control: Insights from the northwest arid regions. *Ecol. Eng.* **2019**, *127*, 75–87. [[CrossRef](#)]
44. Liu, X.; Li, L.; Wang, Q. Land-use change affects stocks and stoichiometric ratios of soil carbon, nitrogen, and phosphorus in a typical agro-pastoral region of northwest China. *J. Soils Sediments* **2018**, *18*, 3167–3176. [[CrossRef](#)]
45. Latruffe, L.; Piet, L. Does land fragmentation affect farm performance? A case study from Brittany, France. *Agric. Syst.* **2014**, *129*, 68–80. [[CrossRef](#)]
46. Zhou, J.; Cao, X. What is the policy improvement of China's land consolidation? Evidence from completed land consolidation projects in Shaanxi Province. *Land Use Pol.* **2020**, *99*, 104847. [[CrossRef](#)]
47. Xu, X.; Xu, Y.; Chen, S. Soil loss and conservation in the black soil region of Northeast China: A retrospective study. *Environ. Sci. Pol.* **2010**, *13*, 793–800. [[CrossRef](#)]
48. Ouyang, W.; Wu, Y.; Hao, Z. Combined impacts of land use and soil property changes on soil erosion in a mollisol area under long-term agricultural development. *Sci. Total Environ.* **2018**, *613–614*, 798–809. [[CrossRef](#)]
49. Gao, J.; Wang, H.; Zuo, L. Spatial gradient and quantitative attribution of karst soil erosion in Southwest China. *Environ. Monit. Assess.* **2018**, *190*, 730. [[CrossRef](#)]

50. Xiao, S.; He, J.; Zeng, C. Soil Chemical Properties under Various Land-Use Types in the Karst Area with a Case Study in Shibing County of China. *J. Chem.* **2021**, *2021*, 5523060. [[CrossRef](#)]
51. Chen, S.; Chen, Y.; Peng, Y. Experimental study on soil erosion characteristics in flooded terraced paddy fields. *Paddy Water Environ.* **2013**, *11*, 433–444. [[CrossRef](#)]
52. Wan, L.; Zhang, Y.; Zhang, X. Comparison of land use/land cover change and landscape patterns in Honghe National Nature Reserve and the surrounding Jiansanjiang Region, China. *Ecol. Indic.* **2015**, *51*, 205–214. [[CrossRef](#)]
53. Ge, X.; Dong, K.; Luloff, A. Correlation between landscape fragmentation and sandy desertification: A case study in Horqin Sandy Land, China. *Environ. Monit. Assess.* **2015**, *188*, 62. [[CrossRef](#)] [[PubMed](#)]
54. Liu, D.; Li, B.; Liu, X. Monitoring land use change at a small watershed scale on the Loess Plateau, China: Applications of landscape metrics, remote sensing and GIS. *Environ Earth. Sci.* **2011**, *64*, 2229–2239. [[CrossRef](#)]
55. Wen, J.; Ying, G. Analysis of landscape ecological security and cultivated land evolution in the Karst mountain area. *Acta Ecol. Sin.* **2018**, *38*, 852–865.
56. Chen, H.; Chen, C.; Zhang, Z. Changes of the spatial and temporal characteristics of land-use landscape patterns using multi-temporal Landsat satellite data: A case study of Zhoushan Island, China. *Ocean Coast Manag.* **2021**, *213*, 105842. [[CrossRef](#)]